# A Broadly Tunable Noise Radar Transceiver on a Silicon Photonic Chip

**Daniel Onori*, José Azaña**
*Institut National de la Recherche Scientifique (INRS-EMT), 800, De La Gauchetière Ouest, Bureau 6900, Montréal, H5A 1K6, Quebec, Canada*
**daniel.onori@emt.inrs.ca*

**Abstract:** We experimentally demonstrate the first on-chip broadly-tunable noise radar transceiver, using silicon photonic technology. By exploiting an innovative and simple lasers' noise referencing architecture, the device shows reconfigurable operation in the range 0.5-35GHz, with antennas-remoting capability. © 2020 The Authors

## 1. Introduction

In next-generation radio detection and ranging (radar) systems for lightweight demanding sensing platforms, the key goal is a low-footprint device able to provide the highest performance in terms of frequency range of operation (0.5-70 GHz and beyond), sensitivity, and antenna remoting [1]. However, due to the intrinsic bandwidth constraints of microwave technology, current solutions operate over a limited number of frequency sub-bands and rely on bulky high-frequency RF synthesizers, signal generators, and cables, thus being unable to reach the desired goals [1].

Over recent decades, microwave photonic technologies have shown attractive features for radar applications, as e.g. ultra-wide bandwidth, very large tunability, and robust antenna remoting capability [2, 3]. However, solution proposed to date still rely in bulky RF components such as a filter bank [2] or an arbitrary waveform generator [3].

With the goal of achieving high performance and low footprint, the first broadly tunable RF scanning receiver on a silicon photonic (SiP) chip was recently demonstrated [4]. The system operates in the 0 - 35 GHz range, avoiding the need for RF filter banks or synthesizers. A novel digital feed-forward (FF) technique was used to cancel the detrimental phase noise introduced by the two free-running, continuous wave lasers (i.e., the optical carrier - OC - and local oscillator - LO -) that feed the system while preserving the RF input signal integrity during the tuning [5].

In this paper, we exploit the receiver architecture concepts in [4] to realize the first, broadly tunable noise radar transceiver on a SiP chip. In more detail, in the transmitter stage, the microwave noise waveform is generated by simply heterodyning the OC laser with the wide-linewidth, broadly tunable LO laser. In the receiver stage, first the OC and LO lasers are used to down-convert to baseband the echo signal backscattered from the target. Then, a digital FF referencing scheme is used to record at intermediate frequency (IF) (*i*) the beat noise between the OC and LO lasers, required to cancel the noise that affects the echo measurement, and (*ii*) the transmitted noise waveform, used as a matched filter for the target detection through cross-correlation. This approach enables simplified on-chip integration and avoids the use of bulky high-frequency RF components. Reconfigurable operation in a frequency range of 0.5 - 35 GHz and a ranging resolution of 0.8 m is demonstrated in an antennas-remoting emulated scenario.

## 2. Principle of operation

The scheme of principle is shown in Fig. 1, bottom side, which is composed by a remote SiP electro-optic converter (SiP EOC) chip, and a central unit. The central unit provides the OC and LO, generated by means of two free-running lasers emitting at frequencies $\nu_{OC}$ and $\nu_{LO}$, with phase noise $\varphi_{OC}(t)$ and $\varphi_{LO}(t)$, respectively. For simplicity of exposition, and without loss of generality, in the following explanation the condition $\varphi_{LO}(t) \gg \varphi_{OC}(t)$ is considered, thus $\varphi_{OC}(t)$ is neglected. First, the central unit sends the OC and LO lasers to the remote SiP EOC through optical fibers. Then, in the EOC, both the OC and LO are split, using two optical Y-junctions (Y in Fig. 1), to be coupled together (white and blue tones, respectively, in Inset A of Fig. 1) in a 3 dB directional coupler (X in Fig. 1) and sent, through the T-port of the X-coupler, to a wideband photodiode ($PD_T$) for heterodyning. At the output of $PD_T$, the noisy RF signal $s_{RF}(t)$ is generated at frequency $f_{RF} = (\nu_{LO} - \nu_{OC})$ with phase noise $\varphi_{LO}(t)$ (blue tone in Inset B). Thereafter, $s_{RF}(t)$ is amplified and transmitted through an antenna (TX in Fig. 1) towards the target. The signal backscattered from the target $s_{BS}(t)$ reaches the receiving antenna (RX) after a time delay $\tau$; it has a center frequency $(\nu_{LO} - \nu_{OC} + f_D)$ and phase noise $\varphi_{LO}(t - \tau)$ (yellow tone in Inset C), i.e., $s_{BS}(t) \propto s_{RF}(t - \tau)\cdot\exp(j\cdot 2\pi\cdot f_D\cdot t)$, where $f_D$ represents the Doppler shift related to the velocity of the target. The EOC transfers the RF input signal $s_{BS}(t)$ to the optical domain by modulating the OC (depicted in Inset D) in a Mach-Zehnder modulator (MZM, see Inset E) and couples the LO with the modulated carrier in a 90° optical hybrid (90°H) coupler. Subsequently, the remote EOC chip transmits the coupled signals back to the signal receiver of the central unit via optical fibers (Inset F), where they are photo-detected by four photodiodes (PDs in balanced configuration), low-pass filtered (LPF), and digitized by two ADCs. The complex envelope signal $s_{BB}$ is calculated in the digital domain from the *I*- and *Q*-channel

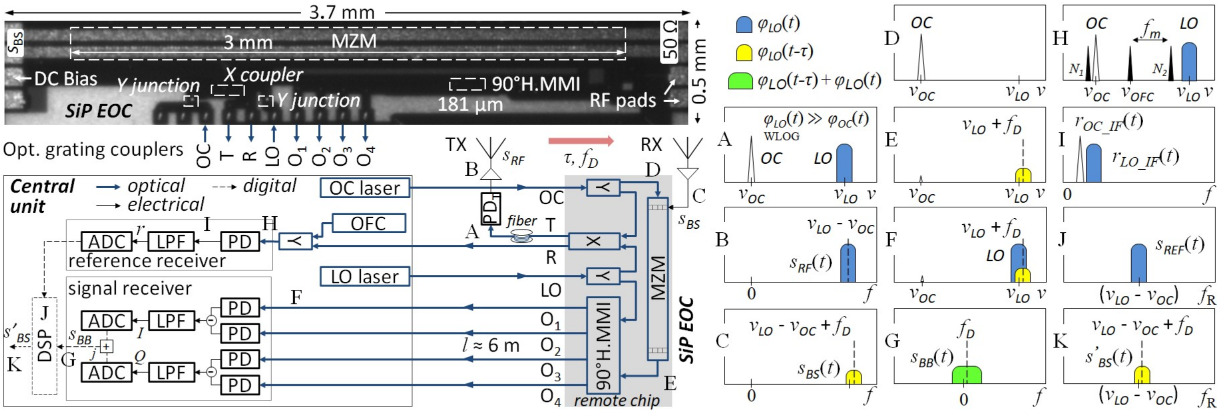


Fig. 1. (Top) Micrograph of the EOC SiP chip. (Bottom) Principle of the SiP-enabled noise radar transceiver (insets: optical or electrical signals at different points in the scheme). ν: optical frequencies; $f$: electrical freq.; $f_R$: reconstructed freq. $O_{1-4}$: optical outputs of the EOC to the signal receiver; R, T: optical output of the EOC to the reference receiver and the transmitting antenna, respectively. WLOG: without loss of generality.

digitized signals, and consists of the received RF signal $s_{BS}(t)$ down-converted to baseband. However, due to the linewidth instability of the free-running lasers, this photonics-assisted RF-to-baseband conversion introduces phase noise, i.e., $\varphi_{LO}(t)$, to the detected signal, a well-known critical problem in this kind of architectures. Therefore, the corrupted baseband signal $s_{BB}(t)$ has a center frequency $f_D$ and phase noise ($\varphi_{LO}(t - \tau) + \varphi_{LO}(t)$) (green tone in Inset G). To mitigate the detrimental effect of this overall noise in the detection process, we use a simple but powerful digital FF cancellation method [4, 5]. In detail, inside the remote EOC, the OC and LO coupled signals (at the R-port of the X-coupler) are sent to the reference receiver of the central unit by means of an optical fiber, where they are coupled with a suitable optical frequency comb (- OFC -, with center frequency $\nu_{OFC}$ and free spectral range $f_m$), using another optical coupler (Inset H), and subsequently heterodyned using a PD. The electrical output $r(t)$ of the PD is digitized through an ADC and consists of the sum of the IF notes ($r_{OC\_IF}(t)$ and $r_{LO\_IF}(t)$ in Inset I) that result from the beating of the OC and LO with the OFC modes closer in frequency (e.g., modes $N_1$ and $N_2$ in Inset H). Afterward, the FF algorithm (implemented using DSP) calculates the reference signal $s_{REF}(t)$, by low-pass filtering and squaring $r(t)$, which provides the differential beat noise between the OC and LO lasers centered at the reconstructed frequency ($f_R$) value of $f_{REF} = (\nu_{LO} - \nu_{OC})$ with phase noise $\varphi_{LO}(t)$ (blue tone in Inset J) [4, 5]. Due to the square-law operation, the reference signal $s_{REF}(t)$ is not affected by the phase noise of the OFC. The output of the FF algorithm $s'_{BS}(t)$ is calculated by multiplying the corrupted baseband signal $s_{BB}(t)$ and the reference signal $s_{REF}(t)$. $s'_{BS}(t)$ corresponds to the reconstructed RF input signal centered at $f_R = (\nu_{LO} - \nu_{OC} + f_D)$, with phase noise $\varphi_{LO}(t - \tau)$ (yellow tone in Inset K), and it is not affected by the RF-to-baseband conversion noise $\varphi_{LO}(t)$ [4, 5]. In addition, $s_{REF}(t)$ correspond to a copy of the RF signal $s_{RF}(t)$ transmitted to the target, and can be used as a matched filter for the successive target detection via cross-correlation. In fact, by calculating the crossambiguity (XA) function $XA(\tau',f')$ between $s'_{BS}(t)$ and $s_{REF}(t)$ [6], an estimate of the range delay $\tau$ and the Doppler frequency shift $f_D$ experienced by the backscattered signal $s_{BS}(t)$, with respect to the transmitted signal $s_{RF}(t)$, can be obtained [6], i.e.,

$$[\tau, f_D] = \arg\max_{\tau',f'}\left\{XA_{s'_{BS}s_{REF}}(\tau',f')\right\},\quad XA_{s'_{BS}s_{REF}}(\tau',f') = \left|\int_{-\infty}^{\infty} s'_{BS}(t)\cdot\exp\{j\cdot 2\pi\cdot f'\cdot t\}\cdot s^{*}_{REF}(t-\tau')\cdot dt\right| \quad (1)$$

## 3. Experimental results

The proposed architecture has been implemented in a laboratory demonstrator. A narrow-linewidth external-cavity laser (ECL) (NetTest, full width at half maximum - FWHM - of 10 kHz) is used for the OC. An ECL in wide-linewidth mode (Ando ECL, FWHM of about 200 MHz) is used as the LO. The SiP EOC chip has been successfully fabricated on silicon-on-insulator (SOI) technology using a multi-project-wafer service. Its footprint is 3.7 x 0.5 mm$^2$. Its micrograph is shown in Fig. 1, upper side. The modulator is a 3-mm long, single drive series push–pull SiP travelling-wave MZM with a 3-dB bandwidth of 40 GHz, based on a lateral PN junction operating near 1550 nm [4]. The small signal $V_\pi$ is 8 V and the insertion loss of the device is on the order of 5 dB. A DC bias voltage of 1 V is applied to the common P-doped region between the two PN junctions, ensuring that they are always reverse biased when the modulator is driven by the maximum driving voltage of 2 $V_{p\text{-}p}$ (10 dBm). The modulator shows linearity performance comparable to that obtained using standard lithium-niobate technology [4]. The 90° optical hybrid coupler is based on a 4x4 multimode interference (MMI) design. It is 181 µm long and 10 µm wide. [4]. The Y-junctions and the X-coupler are library components [4]. In the central unit, the OFC generator is implemented with a cascade of two intensity and two phase lithium-niobate modulators driven by an RF clock at a frequency

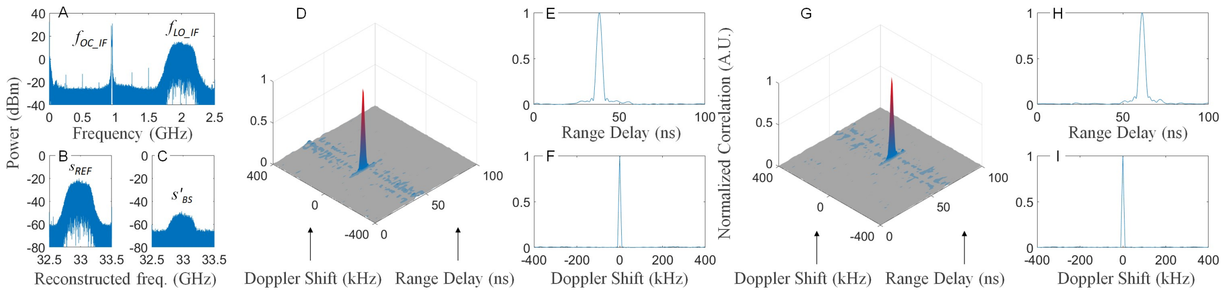


Fig. 2. (A, B, and C) PSDs of the digitized signals $r(t)$, $s_{REF}(t)$, and $s'_{BS}(t)$, respectively. (D, E, and F) Plot of the crossambiguity function and its cuts at the maximum value, respectively, when the emulated target delay $\tau = 38.3$ ns and $f_{RF} = 33$ GHz. (G, H, and I) Plot of the crossambiguity function and its cuts when $\tau = 61.2$ ns and $f_{RF} = 8$ GHz.

$f_m = 5$ GHz [4, 5]. The sampling frequency of the ADCs is $f_s = 5$ Gsps. The acquisition time $T_{acq}$ is set to 100 µs (resolution bandwidth - RBW = 10 kHz). An antennas-remoting scenario is emulated by connecting the EOC chip with the central unit using six-meter-long optical fibers (see Fig. 1).

In this preliminary test, the target range is emulated using fiber-optic patch cords before the $PD_T$ in the transmitter (see *fiber* in Fig.1), and connecting the $PD_T$ output to the RF input of the MZM, by using a 30 dB RF amplifier and a 40 dB RF attenuator to simulate the radar propagation loss. So, a target range of around 7.66 m is emulated introducing a fiber-optic patch cord. As a first example, the detection can be achieved by setting the LO's frequency $\nu_{LO}$ at around 33 GHz from the OC's frequency $\nu_{OC}$ ($\nu_{LO} - \nu_{OC} \approx 33$ GHz, $N_2 - N_1 = 6$). This way an RF noise signal is generated at $f_{RF} \approx 33$ GHz with a bandwidth of ~200 MHz. The power spectral density (PSD) of the acquired signals $r(t) = r_{OC\_IF} + r_{LO\_IF}$ is depicted in Fig.2-A, showing the $r_{OC\_IF}$ and $r_{LO\_IF}$ beat noise waveforms down-converted at around $f_{OC\_IF} = 1$ and $f_{LO\_IF} = 2$ GHz, respectively (corresponding to the illustration in Inset I of Fig. 1). Fig. 2-B depicts the power spectrum of the reference signal $s_{REF}$, showing the lasers' beat noise signal centered at the reconstructed frequency ($f_R$) $f_{REF} = \nu_{LO} - \nu_{OC} = f_{LO\_IF} + f_{OC\_IF} + (N_2 - N_1) \cdot f_m \approx 33$ GHz (corresponding to the blue tone in Inset J of Fig. 1). The PSD of the reconstructed backscattered signal, $s'_{BS}(t)$, is also centered at around 33 GHz ($f_D = 0$) and depicted in Fig. 2-C (see the yellow tone in Inset K of Fig. 1). Fig. 2-D depicts the output of the XA function defined in Eq. 1: the measure of its peak position provides the range $R$ and velocity $V$ of the target, i.e., $\tau = 38.3$ ns ($R = c \cdot \tau = 7.66$ m, with $c \approx 2 \cdot 10^8$ speed of light in fiber) and $f_D = 0$ ($V = f_D \cdot c / 2 / f_{REF} = 0$). The estimated values are in excellent agreement with those of the target. Fig. 2-E and -F depict the plot of the XA function cuts [6] at the Doppler value $f_D$ and delay value $\tau$, respectively, and show that the range resolution is around 0.8 m (the FWHM of the delay measure equals 4 ns, consistently with the 200-MHz bandwidth of the LO laser), while the frequency (and also velocity) resolution is limited by the RBW = 10 kHz. As a second example aimed at illustrating the frequency tuning capabilities of the transceiver, Fig. 2-G, -H, and -I show similar performance in the measurement results when a target range delay of ~ 61.2 ns ($R = 12.24$ m) is emulated, and the LO's frequency $\nu_{LO}$ is set at around 8 GHz from the OC's frequency $\nu_{OC}$ (i.e., the transceiver operates at $f_{RF} = f_{REF} = \nu_{LO} - \nu_{OC} \approx 8$ GHz).

## 4. Conclusions

In conclusion, this paper presents the experimental demonstration of the first wideband, broadly tunable noise radar transceiver on a silicon photonic chip. The reported SOI architecture has been successfully fabricated using a multi-project-wafer service, and it is based on an innovative and simple digital FF noise referencing scheme that avoids the use of bulky RF waveform generators and synthesizers; in sharp contrast, this scheme allows for the use of low cost components with a small size, weight, and power footprint. By tuning the emission frequency of the LO laser, a reconfigurable frequency operation up to 35 GHz and a ranging resolution of 0.8 m is demonstrated, limited by the RF input bandwidth of the SiP MZM and the linewidth of the LO laser, respectively. Moreover, because the interferometric structures inside the remote EOC are implemented monolithically through photonic integration, the system is insensitive to the mechanical vibrations of the environment (even in antennas-remoting applications).

Therefore, the proposed on-chip transceiver enables meeting the requirements of next-generation lightweight radars, in terms of performance (e.g., broad tunability), small footprint, low cost, and antennas-remoting capability.

## 5. References

[1] M. Richards et al., "Principles of Modern Radar: Basic Principles", SciTech Publishing, ISBN: 1891121529.
[2] P. Ghelfi et al., "A fully photonics-based coherent radar system", Nature, doi: 10.1038/nature13078.
[3] S. L. Z. Cui et al., "Chip-based photonic radar for high-resolution imaging", arXiv:1905.12802.
[4] D. Onori et al., "An RF Scanning Receiver on a Silicon Photonic Chip", accepted at Microwave Phot. conf., Postdeadline, Ottawa, CA, 2019.
[5] D. Onori et al., Microwave Photonics conference, Toulouse, France, October, 2018, doi: 10.1109/MWP.2018.8552849.
[6] 'ambgfun - Ambiguity and crossambiguity function', https://www.mathworks.com/help/phased/ref/ambgfun.html, accessed 19 October 2019.